



HAL
open science

Three-Qubit Operators, the Split Cayley Hexagon of Order Two and Black Holes

Peter Levay, Metod Saniga, Peter Vrana

► **To cite this version:**

Peter Levay, Metod Saniga, Peter Vrana. Three-Qubit Operators, the Split Cayley Hexagon of Order Two and Black Holes. *Physical Review D*, 2008, 78, 124022 [16 p.]. 10.1103/PhysRevD.78.124022 . hal-00315306v2

HAL Id: hal-00315306

<https://hal.science/hal-00315306v2>

Submitted on 11 Sep 2008

HAL is a multi-disciplinary open access archive for the deposit and dissemination of scientific research documents, whether they are published or not. The documents may come from teaching and research institutions in France or abroad, or from public or private research centers.

L'archive ouverte pluridisciplinaire **HAL**, est destinée au dépôt et à la diffusion de documents scientifiques de niveau recherche, publiés ou non, émanant des établissements d'enseignement et de recherche français ou étrangers, des laboratoires publics ou privés.

Three-Qubit Operators, the Split Cayley Hexagon of Order Two and Black Holes

Péter Lévay,¹ Metod Saniga² and Péter Vrana¹

¹Department of Theoretical Physics, Institute of Physics, Budapest University of Technology and Economics, H-1521 Budapest, Hungary
and

²Astronomical Institute, Slovak Academy of Sciences
SK-05960 Tatranská Lomnica, Slovak Republic

(11 September 2008)

Abstract

The set of 63 real generalized Pauli matrices of three-qubits can be factored into two subsets of 35 symmetric and 28 antisymmetric elements. This splitting is shown to be completely embodied in the properties of the Fano plane; the elements of the former set being in a bijective correspondence with the 7 points, 7 lines and 21 flags, whereas those of the latter set having their counterparts in 28 anti-flags of the plane. This representation naturally extends to the one in terms of the split Cayley hexagon of order two. 63 points of the hexagon split into 9 orbits of 7 points (operators) each under the action of an automorphism of order 7. 63 lines of the hexagon carry three points each and represent the triples of operators such that the product of any two gives, up to a sign, the third one. Since this hexagon admits a full embedding in a projective 5-space over $GF(2)$, the 35 symmetric operators are also found to answer to the points of a Klein quadric in such space. The 28 antisymmetric matrices can be associated with the 28 vertices of the Coxeter graph, one of two distinguished subgraphs of the hexagon. The $PSL_2(7)$ subgroup of the automorphism group of the hexagon is discussed in detail and the Coxeter sub-geometry is found to be intricately related to the E_7 -symmetric black-hole entropy formula in string theory. It is also conjectured that the full geometry/symmetry of the hexagon should manifest itself in the corresponding black-hole solutions. Finally, an intriguing analogy with the case of Hopf sphere fibrations and a link with coding theory are briefly mentioned.

PACS: 02.40.Dr, 03.65.Ud, 03.65.Ta, 03.67.-a, 04.70.-s

Keywords: Three-Qubit Pauli Group — Fano Plane — Generalized Hexagon of Order Two
— E_7 -Symmetric Stringy Black Holes

1 Introduction

Entanglement and geometry are key concepts in contemporary theoretical physics. The first can be regarded as the “characteristic trait of quantum theory”, the second as the basic unifying agent in explaining the fundamental forces. A vital combination of these concepts shows up in two seemingly unrelated fields, quantum information and quantum gravity. The basic goal in quantum information is understanding entanglement in geometric terms, and in quantum gravity the understanding of the structure of the Bekenstein-Hawking entropy of certain stringy black hole solutions. Recently, in a series of papers a striking correspondence has been established between this two apparently separate fields [1]–[7]. For the intriguing mathematical coincidences underlying this correspondence M. J. Duff and S. Ferrara coined the term “Black Hole Analogy”. The basic correspondence of the analogy is the one between the black hole entropy formula of certain stringy black hole solutions on one hand and entanglement measures for qubit and qutrit systems on the other. The archetypical example [1] of such a correspondence is the one concerning the 8-charge STU black hole of $N = 2$, $D = 4$ supergravity [8, 9]. The entropy formula in this case is of the form

$$S = \frac{\pi}{2} \sqrt{\tau_{ABC}}, \quad (1)$$

where τ_{ABC} is the so called three-tangle [10], an entanglement measure characterizing entangled three-qubit systems A, B and C . Later works [2, 4, 5] have revealed that the most general type of stringy black hole solutions with 56 charges occurring within the context of $N = 8, D = 4$ supergravity also display this correspondence. Here the $E_{7(7)}$ symmetric black hole entropy formula is

$$S = \frac{\pi}{2} \sqrt{\tau_{ABCDEFG}}, \quad (2)$$

where $\tau_{ABCDEFG}$ is an entanglement measure characterizing the *tripartite entanglement of seven qubits*. This measure is related to the unique quartic Cartan invariant for the fundamental representation of the exceptional group $E_{7(7)}$, and to the discrete geometry of the Fano plane. Truncations of the discrete *U-duality* group $E_7(\mathbf{Z})$ have been connected to truncations of the Fano plane to its points, lines and quadrangles [5]. This result can be regarded as the first indication that discrete geometric ideas could play a key role in a quantum-entanglement-based understanding of duality symmetries. As a latest development, a physical basis for the Black Hole Analogy in the special case of the STU model has recently been revealed. It has been shown that the qubits occurring in the analogy can be realized as wrapped intersecting D3-branes [7].

It has become obvious from the very beginning that the quantum information theoretic basis for the black hole correspondence rests on the very special geometric properties of few qubit systems [3]. Indeed, in the quantum entanglement literature it has become common wisdom that the special geometry of one, two and three-qubit systems can naturally be related to Hopf fibrations related to the complex numbers, quaternions and octonions, respectively [11]–[13]. These approaches to few qubit systems studied the geometry of entanglement via looking at the geometry of the corresponding multi-qubit *Hilbert space*. An alternative approach to understanding entanglement in geometric terms is provided by the one of studying the geometry of the *algebra of observables* with special operators (e.g., CNOT operations) creating and destroying entanglement by acting on it. In particular, it proved to be of fundamental importance to look at the structure of the so-called Pauli group on few qubits. This group is of utmost importance in the field of fault tolerant quantum computation and stabilizer codes. The algebra of the generalized Pauli group of N -qubit systems has also remarkable discrete geometric properties, being completely embodied in the so-called *symplectic polar spaces* of order two and rank N [14]–[17].

Although the appearance of few qubit (and qutrit) entangled systems related to discrete geometric structures provided an additional insight into the structure of stringy black hole solutions, some basic points still remained obscure. In particular, the entangled state characterizing the tripartite entanglement of seven qubits is not the one occurring in conventional quantum information theory. This state is *not* an element of any subspace of the Hilbert space on seven qubits. Indeed, it has been shown that it is an element of a 56-dimensional subspace of seven qutrits [4]. Moreover, a special role of three-qubit systems repeatedly showing up in these systems hints at an alternative structure lurking behind the scene.

Motivated by the desire to eliminate such shortcomings, in this paper we initiate an observable-based understanding of the Black Hole Analogy. Our basic object of scrutiny is the discrete geometry of the Pauli group of three-qubits. Although the corresponding geometry of two-qubits, which is that of the *generalized quadrangle of order two* [15, 16], has already been worked out in detail, a similar comprehensive analysis for three-qubits is still missing. The main body of the paper is, therefore, devoted to a detailed study of the geometry of the *real* operators of this group. The principal result of this part is an explicit demonstration of the fact that the 63 real operators of the Pauli group can be mapped bijectively to the points of the so-called *split Cayley hexagon of order two*. The last part of the paper is devoted to establishing an explicit correspondence between a sub-geometry of this hexagon and the $E_{7(7)}$ symmetric black hole entropy formula. The symmetry of this (Coxeter-graph-based) geometry turns out to be related to a $PSL_2(7)$ subgroup of the full *U-duality* group. In order to relate our observable based approach to the seven-qubit Hilbert space based one [4, 5], we provide the basic dictionary relating these two approaches. Finally, we also conjecture that the geometry and symmetry of the Hexagon in its full generality should manifest itself at the level of such black hole solutions. Our hope is that this new

approach will initiate further investigations to fill in the missing gaps, and to explore the possible physical consequences.

The paper is organized as follows. First, we shall demonstrate that the algebra of our 63 generalized Pauli matrices is fully encoded in the properties of the Fano plane and its dual (Sec. 2). Then, by employing its automorphism of order 7 (Sec. 3), we shall illustrate in many details how this encoding naturally and straightforwardly translates into the properties and characters of the points/lines of this split Cayley hexagon and one of its representation inside a projective 5-space (Sec. 4). Next, a quite in-depth examination of $PSL_2(7)$, a subgroup of the full automorphism group of the hexagon, will follow (Sec. 5). Finally, the Coxeter graph, one of two most important sub-configurations living within our hexagon (the other being the incidence graph of the Fano plane — the Heawood graph), will be given close scrutiny and shown to be intricately linked with the E_7 -symmetric black-hole entropy formula in string theory (Sec. 6). The paper will be finished by a brief discussion of an intriguing analogy with Hopf sphere fibrations and an outline of a worth-exploring link with coding theory.

2 Real operators on three-qubits and the Fano plane

Let us define the following set of 2×2 matrices

$$I = \begin{pmatrix} 1 & 0 \\ 0 & 1 \end{pmatrix}, \quad X = \begin{pmatrix} 0 & 1 \\ 1 & 0 \end{pmatrix}, \quad Y = \begin{pmatrix} 0 & 1 \\ -1 & 0 \end{pmatrix}, \quad Z = \begin{pmatrix} 1 & 0 \\ 0 & -1 \end{pmatrix}. \quad (3)$$

Notice that except for Y these are the 2×2 identity and the usual Pauli spin matrices. They are symmetric except for Y which is antisymmetric. We note that the set $\mathcal{M} = \{\pm I, \pm X, \pm Y, \pm Z\}$ consists of the *real* operators of the Pauli group acting on a single qubit.

We consider three-qubit systems with Hilbert space $\mathcal{H} \equiv \mathbf{C}^2 \otimes \mathbf{C}^2 \otimes \mathbf{C}^2$ on which the Kronecker (tensor) product of three 2×2 matrices $A \otimes B \otimes C$ is defined in the usual way. Here we refer to A , B and C as the matrices acting on the first, second and third qubit, respectively. Let us now assume that $A, B, C \in \mathcal{M}$ and introduce the shorthand notation ABC for their Kronecker product; hence, for example, we have

$$ZYX \equiv Z \otimes Y \otimes X = \begin{pmatrix} Y \otimes X & 0 \\ 0 & -Y \otimes X \end{pmatrix} = \begin{pmatrix} 0 & X & 0 & 0 \\ -X & 0 & 0 & 0 \\ 0 & 0 & 0 & -X \\ 0 & 0 & X & 0 \end{pmatrix}. \quad (4)$$

Notice that the 8×8 matrices containing an *odd* number of Y 's are *antisymmetric*, whilst those comprising an *even* number of Y 's are *symmetric*; thus, for example, ZYX is an antisymmetric matrix, but IYY and XZX are symmetric ones.

Up to a sign, we have altogether $4^3 = 64$ distinct 8×8 matrices. After omitting the identity $III \equiv I \otimes I \otimes I$ we are left with 63 matrices of which 28 are antisymmetric and 35 symmetric. In the space of symmetric 8×8 matrices we consider the following two seven-element sets

$$\mathcal{L} \equiv \{IIX, IXI, IXX, XII, XIX, XXI, XXX\} \quad (5)$$

and

$$\mathcal{P} \equiv \{IIZ, IZI, IZZ, ZII, ZIZ, ZZI, ZZZ\} \quad (6)$$

to have a special status. We will see soon that the elements of these sets can be associated with the *points* (\mathcal{P}) and *lines* (\mathcal{L}) of the projective plane of order two, the Fano plane. Here we simply observe that the elements of these sets are pairwise commuting.

Our next step is to create a multiplication table by taking the elements of the set \mathcal{L} to label the rows and those of the set \mathcal{P} to label the columns of a 7×7 array whose entries are, *up to a sign*, the (ordinary matrix) products of the corresponding elements. After carrying

Table 1: The matrix products between the operators from the two distinguished sets.

Lines/Points	ZZI	ZII	ZZZ	IZI	IZZ	ZIZ	IIZ
IIX	ZZX	ZIX	<u>ZZY</u>	IZX	<u>IZY</u>	<u>ZIY</u>	<u>$I IY$</u>
IXX	<u>ZYX</u>	ZXX	ZYY	<u>IYX</u>	IYY	<u>ZXY</u>	<u>IXY</u>
XIX	<u>YZX</u>	<u>YIX</u>	YZY	XZX	<u>XZY</u>	YIY	<u>XIY</u>
XII	<u>YZI</u>	<u>YII</u>	<u>YZZ</u>	XZI	XZZ	<u>YIZ</u>	XIZ
XXX	YYX	<u>YXX</u>	<u>YYY</u>	<u>XYX</u>	$XY Y$	YXY	<u>XXY</u>
IXI	<u>ZYI</u>	ZXI	<u>ZYZ</u>	<u>IYI</u>	<u>IYZ</u>	ZXZ	IXZ
XXI	YYI	<u>YXI</u>	YYZ	<u>XYI</u>	<u>XYZ</u>	<u>YXZ</u>	XXZ

out all the calculations, we notice that the 21 symmetric and the 28 antisymmetric matrices from this 7×7 array reveal an incidence structure reminiscent of the one of the Fano plane. More precisely, we find three pairwise commuting symmetric and four pairwise commuting antisymmetric combinations occurring in both each row and each column. Moreover, any two elements such that one belongs to the symmetric and the other to the antisymmetric set (lying in a particular row or column) are anti-commuting (not commuting). Next, if we look at the pattern of the location of symmetric combinations pertaining to different rows and columns we obtain the same structure we get by looking at the incidence structure of points and lines of the Fano plane and its dual.

Let us explicitly see how this works. After a particular ordering of the elements of the sets \mathcal{P} and \mathcal{L} we can group the remaining 49 matrices in the manner as depicted in Table 1. In the first row (IIX) we have pairwise commuting symmetric combinations in columns 1, 2, and 4 (i.e., in the columns labelled by the triples ZZI, ZII , and IZI), and pairwise commuting antisymmetric ones in columns 3, 5, 6, and 7 (that is, in ZZZ, IZZ, ZIZ , and IIZ — the corresponding entries being underlined). Looking at the other rows we readily notice a *cyclic shift* of this pattern: $(124) \rightarrow (235) \rightarrow (346) \rightarrow (457) \rightarrow (561) \rightarrow (672) \rightarrow (713)$. It represents no difficulty to check that this pattern is embodied in the structure of the Fano plane, as shown in Fig. 1, left; here, the grey numbers (points) respectively black ones (lines) from 1 to 7 label the columns respectively rows, together with the respective matrices of the two special sets, of Table 1. Dually, in the first column (ZZI) we have pairwise commuting symmetric combinations in rows 5, 7, and 1 (XXX, XXI, IIX), and pairwise commuting antisymmetric ones in rows 2, 3, 4, and 6 (IXX, XIX, XII , and IXI). Now the cyclically shifted pattern looks as follows $(134) \rightarrow (245) \rightarrow (356) \rightarrow (467) \rightarrow (571) \rightarrow (612) \rightarrow (723)$, being reproduced by the geometry of the dual Fano plane (Fig. 1, right).

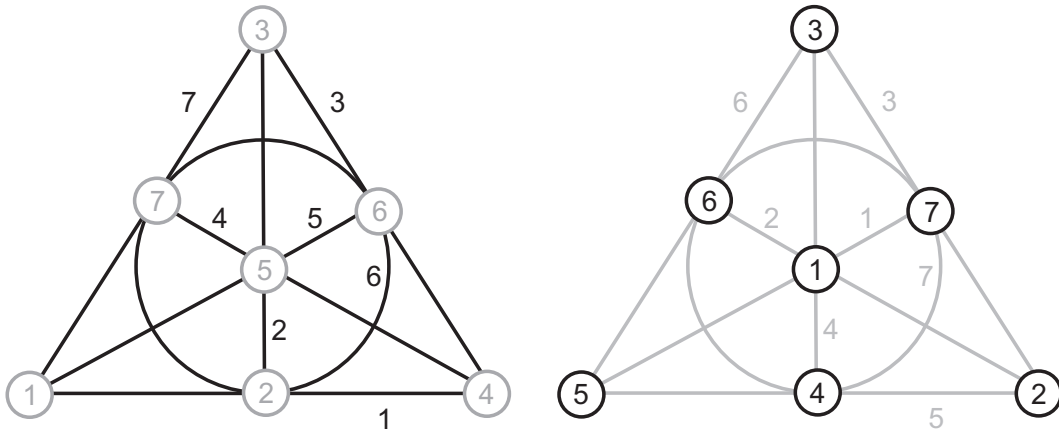


Figure 1: The Fano plane and its dual as the fundamental building blocks of the three-qubit Pauli group algebra.

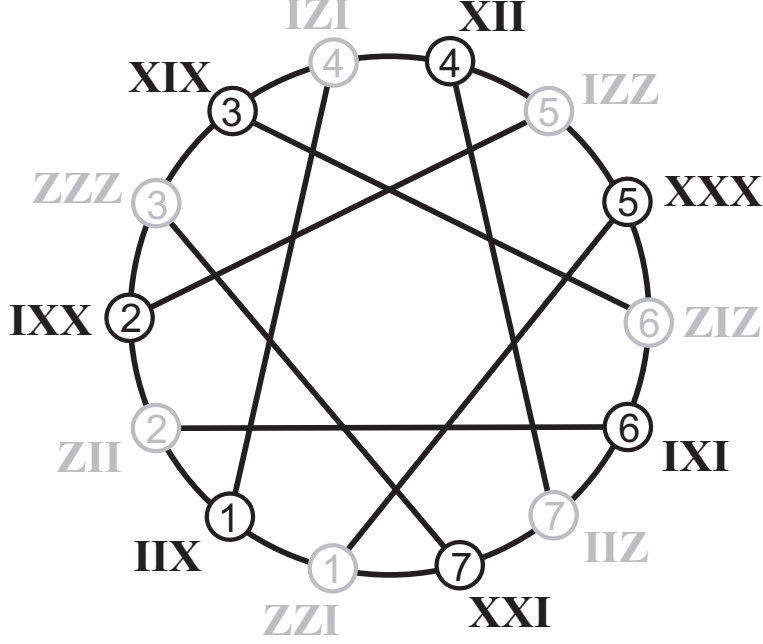


Figure 2: The algebra of the operators from the two distinguished sets in terms of the incidence graph of the Fano plane.

This dual view of the operators' algebra can be cast into a single compact form by employing the incidence graph of the Fano plane, also known as the Heawood graph (Fig. 2). This graph consists of 14 vertices corresponding to the seven points (grey circles) and seven lines (black circles) of the Fano plane, with two vertices (of different shading) being adjacent if they correspond to a point and a line such that the point is contained in the line.

From the above-outlined picture we observe that the symmetric combinations correspond to the flags (a line taken together with a point lying on it) and the antisymmetric ones to the antiflags (a line and a point *not* lying on that line) of the Fano plane. Taken together with the sets \mathcal{P} and \mathcal{L} whose elements label the points and the lines, we see that *all* 63 nontrivial matrices forming a subset of the generalized three-qubit Pauli group can *completely* be described in geometrical terms related to the structure of the Fano plane. This is a very important finding because there exists a remarkable unique finite geometry whose properties can be fully derived from the structure of the Fano plane *alone*, viz. a thick generalized polygon called split Cayley hexagon [18]–[22]. In order to show that this geometry indeed mimics all the essential features of the commutation algebra of our generalized Pauli matrices, one more piece of three-qubit mathematics must be given a careful inspection and properly understood — automorphisms of order 7.

3 Automorphism of order seven and its orbits

To this end in view, let us denote by α the following permutation: (1234567); this is obviously of order seven. We would like to find an 8×8 representation of α which permutes cyclically the elements of the ordered sets \mathcal{P} and \mathcal{L} we used to label the rows and columns of Table 1. We have to find, in particular, an 8×8 matrix $\mathcal{D}(\alpha)$ with the property $(\mathcal{D}(\alpha))^7 = III$ that acts on the elements of \mathcal{P} and \mathcal{L} by conjugation in the following way

$$\mathcal{D}(\alpha) : IIX \mapsto IXX \mapsto XIX \mapsto XII \mapsto XXX \mapsto IXI \mapsto XXI \mapsto IIX \mapsto \dots, \quad (7)$$

$$\mathcal{D}(\alpha) : ZZI \mapsto ZII \mapsto ZZZ \mapsto IZI \mapsto IZZ \mapsto ZIZ \mapsto IIZ \mapsto ZZI \mapsto \dots, \quad (8)$$

where

$$\mathcal{D}(\alpha)^{-1} IIX \mathcal{D}(\alpha) = IXX, \quad \mathcal{D}(\alpha)^{-1} IXX \mathcal{D}(\alpha) = XIX, \quad \dots \quad (9)$$

Such a matrix is of the form

$$\mathcal{D}(\alpha) \equiv \begin{pmatrix} P & Q & 0 & 0 \\ 0 & 0 & Q & P \\ 0 & 0 & QX & PX \\ PX & QX & 0 & 0 \end{pmatrix}, \quad P = \begin{pmatrix} 1 & 0 \\ 0 & 0 \end{pmatrix}, \quad Q = \begin{pmatrix} 0 & 0 \\ 0 & 1 \end{pmatrix}. \quad (10)$$

Now let us look at the action of $\mathcal{D}(\alpha)$ on 21 symmetric matrices labelling the flags and 28 antisymmetric matrices labelling the anti-flags of the Fano plane. We find exactly seven orbits of seven elements each. The aggregate of 21 symmetric matrices splits into three orbits. One of them is represented by the elements located on the main diagonal of Table 1,

$$\mathcal{D}(\alpha) : ZZX \mapsto ZXX \mapsto YZY \mapsto XZI \mapsto XYY \mapsto ZXZ \mapsto XXZ \mapsto ZZX \mapsto \dots, \quad (11)$$

the other two being represented by the matrices sitting at the positions shifted rightward by one column and/or three columns from the main diagonal in a cyclic manner, namely

$$\mathcal{D}(\alpha) : ZIX \mapsto ZYY \mapsto XZX \mapsto XZZ \mapsto YXY \mapsto IXZ \mapsto YZI \mapsto ZIX \mapsto \dots, \quad (12)$$

and

$$\mathcal{D}(\alpha) : IZX \mapsto IYY \mapsto YIY \mapsto XIZ \mapsto YYX \mapsto ZXI \mapsto YYZ \mapsto IZX \mapsto \dots, \quad (13)$$

respectively. The set of 28 antisymmetric matrices factors into four orbits; the elements of all of them are located above the main diagonal shifted from it by two, four, five and six columns. Their explicit forms read

$$\mathcal{D}(\alpha) : ZZY \mapsto IYX \mapsto XZY \mapsto YIZ \mapsto XXY \mapsto ZYI \mapsto YXI \mapsto ZZY \mapsto \dots, \quad (14)$$

$$\mathcal{D}(\alpha) : IZY \mapsto ZXY \mapsto XIY \mapsto YZI \mapsto YXX \mapsto ZYZ \mapsto XYI \mapsto IZY \mapsto \dots, \quad (15)$$

$$\mathcal{D}(\alpha) : ZIY \mapsto IXY \mapsto YZX \mapsto YII \mapsto YYY \mapsto IYI \mapsto XYZ \mapsto ZIY \mapsto \dots, \quad (16)$$

and

$$\mathcal{D}(\alpha) : IYY \mapsto ZYX \mapsto YIX \mapsto YZZ \mapsto XYX \mapsto IYZ \mapsto YXZ \mapsto IYY \mapsto \dots, \quad (17)$$

respectively.

It is important to realize here that the action of $\mathcal{D}(\alpha)$ on the three-qubit Hilbert space changes, in general, the entanglement type (see, e. g., the SLOCC classes a particular state belongs to [23]). This can be demonstrated by expressing $\mathcal{D}(\alpha)$ in terms of three-qubit CNOT operations, which are well known to create or destroy entanglement [24]. One possible way to express $\mathcal{D}(\alpha)$ in terms of CNOT operations is

$$\mathcal{D}(\alpha) = (C_{12}C_{21})(C_{12}C_{31})C_{23}(C_{12}C_{31}). \quad (18)$$

Here, the explicit forms of the three-qubit CNOT operations are [24]

$$C_{12} = \begin{pmatrix} I & 0 & 0 & 0 \\ 0 & I & 0 & 0 \\ 0 & 0 & 0 & I \\ 0 & 0 & I & 0 \end{pmatrix}, \quad C_{21} = \begin{pmatrix} I & 0 & 0 & 0 \\ 0 & 0 & 0 & I \\ 0 & 0 & I & 0 \\ 0 & I & 0 & 0 \end{pmatrix}, \quad (19)$$

$$C_{23} = \begin{pmatrix} I & 0 & 0 & 0 \\ 0 & X & 0 & 0 \\ 0 & 0 & I & 0 \\ 0 & 0 & 0 & X \end{pmatrix}, \quad C_{31} = \begin{pmatrix} P & 0 & Q & 0 \\ 0 & P & 0 & Q \\ Q & 0 & P & 0 \\ 0 & Q & 0 & P \end{pmatrix}, \quad (20)$$

with the first index relating to the location of the control bit and the second one to the target.

The fourth orbit of antisymmetric matrices, Eq. (17), has several noteworthy properties. The seven operators of this orbit are pairwise anti-commuting. Since the square of each of these operators is $-III$, replacing Y by $\sigma_2 = -iY$ we get the matrices forming a representation of a seven dimensional Clifford algebra,

$$\{i\Gamma_1, i\Gamma_2, i\Gamma_3, i\Gamma_4, i\Gamma_5, i\Gamma_6, i\Gamma_7\} = \{IIY, ZYX, YIX, YZZ, XYX, IYZ, YXZ\} \quad (21)$$

$$\Gamma_j\Gamma_k + \Gamma_k\Gamma_j = 2\delta_{jk}\mathbf{1}, \quad \mathbf{1} \equiv III, \quad j, k = 1, 2, \dots, 7. \quad (22)$$

It is then straightforward to check that the remaining three orbits of antisymmetric matrices can be generated as the commutators of the form $\frac{1}{2}[\Gamma_j, \Gamma_k]$. This shows that the remaining 21 matrices, Eqs. (14)–(16), form the irreducible spinor representation of an $so(7)$ algebra. Hence, the totality of 28 antisymmetric matrices $S_{0k} = \frac{i}{2}\Gamma_k$ and $S_{jk} = \frac{1}{4}[\Gamma_j, \Gamma_k]$, associated with the anti-flags of the Fano plane, form the generators of one of the irreducible spinor representations of the $so(8)$ algebra with the generators S_{jk} giving rise to the $so(7)$ subalgebra.

Finally, we will notice that the elements of our specific fourth orbit can be used to label the points of an *oriented* dual Fano plane. That is, instead of the ordered set $\mathcal{L} = \{IIX, IXX, XIX, XII, XXX, IXI, XXI\}$ labelling the rows of Table 1 and the points of Fig. 1, right, we can use the ordered set $\mathcal{L}' = \{IIY, ZYX, YIX, YZZ, XYX, IYZ, YXZ\}$. Since, for example, the result of the multiplication $(XYX)(YZZ)(ZYX)$ (reading this from left to right) gives $+IZZ$, we can endow the line labelled by IZZ with an arrow pointing from left to right. Due to the above-described Clifford property, all even permutations of this triple product result in $+IZZ$, while odd ones yield $-IZZ$. Proceeding this way, every line of the dual Fano plane can be given a unique orientation — as illustrated in Fig. 3. Making one step further and employing the following correspondence between the unit octonions and the elements of our special set, $\{e_1, e_2, e_3, e_4, e_5, e_6, e_7\} \leftrightarrow \{XYX, YZZ, YIX, ZYX, IIY, YXZ, IYZ\}$, Fig. 3 is found to be identical with a simple mnemonic for the products of the unit octonions [25]. Note, however, that for the octonions we have, for example, $e_1e_2 = e_4$, but in our case $(XYX)(YZZ) \neq ZYX$. So, the set \mathcal{L}' can only be used to mimic the signs occurring in the octonionic multiplication table.

At this point we have at hand all the necessary technicalities to reveal the smallest split Cayley hexagon lurking behind the core algebraic properties of the 63 nontrivial real operators of the Pauli group on three qubits.

4 Core geometry: the smallest split Cayley hexagon

A finite generalized n -gon \mathcal{G} of order (s, t) is a point-line incidence geometry satisfying the following three axioms [18]–[22]:

- (A1) Every line contains $s + 1$ points and every point is contained in $t + 1$ lines.
- (A2) \mathcal{G} does not contain any ordinary k -gons for $2 \leq k < n$.
- (A3) Given two points, two lines, or a point and a line, there is at least one ordinary n -gon in \mathcal{G} that contains both objects.

From the definition it is obvious that the dual of a generalized n -gon is also a generalized n -gon. If $s = t$ we say that the n -gon is of order s . An ordinary n -gon is the unique generalized n -gon of order 1. A generalized polygon is called *thick* if every point is contained in at least three lines and every line contains at least three points, i. e., if $s, t \geq 2$. The Fano plane is the unique generalized triangle of order two. There exists a unique (self-dual) generalized quadrangle of order two; this object that we already spoke about in the introduction plays a crucial role in the description of the generalized Pauli group of two qubits [15, 16]. It can be easily checked that the Heawood graph (the incidence graph of the Fano plane, Fig. 2) is the generalized hexagon of order $(1, 2)$. There are also two generalized hexagons of order two, the so-called split Cayley hexagon and its dual [18]–[22], [26]. Our main concern here

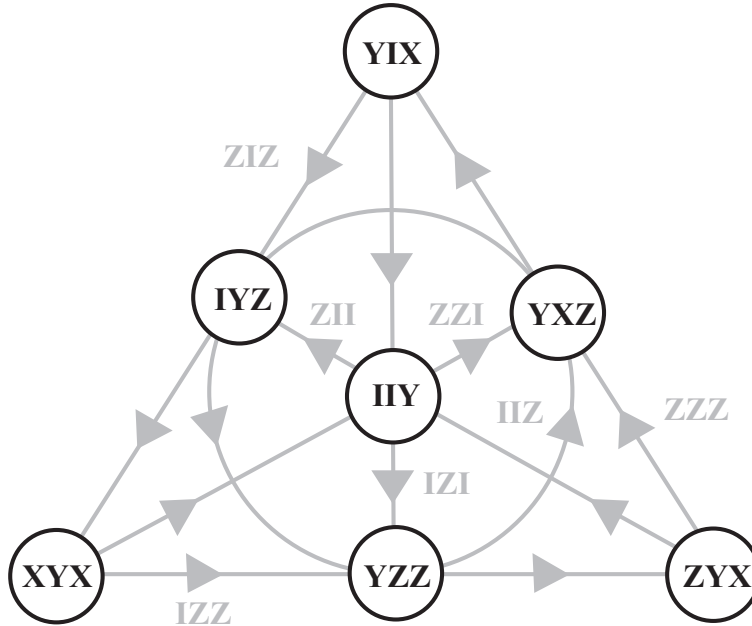


Figure 3: The oriented dual Fano plane.

is the former one, also known as the $G_2(2)$ hexagon because the Chevalley group $G_2(2)$ is basically its automorphism group and in what follows simply referred to as the Hexagon. It has 63 points and 63 lines; every point is contained in three lines and every line contains three points. One of its stunning pictures created by the method of “finite pottery” [18, 19] is reproduced in Fig. 4.

Since the Pauli group on three qubits contains 63 nontrivial real operators and the Hexagon is endowed with 63 points/lines as well, one is immediately tempted to conjecture that the two objects have something to do with each other. This conjecture is indeed fairly justified by the facts that the geometry behind the commutation algebra of the *complex* three-qubit Pauli group is that of the so-called symplectic polar space of order two and rank three [14, 17] and that our Hexagon lives fully embedded in this space [27]. Given the seven-fold symmetry of the Hexagon under which its 63 points are organized precisely into 9 orbits with 7 elements each (see Fig. 4) and the fact that we have an automorphism $\mathcal{D}(\alpha)$ of order seven acting on 63 operators of the Pauli group which gives rise to the same orbit structure, all we have to do is to find the algebraic counterpart of the basic incidence relations of the Hexagon and verify the remaining structural relations.

In order to carry out this program, we first notice that the Hexagon contains a copy of the Heawood graph (the sub-configuration in Fig. 4 consisting of the yellow and brown circles and the corresponding dark grey lines — compare with Fig. 2). According to our labelling scheme in terms of the ordered sets \mathcal{P} and \mathcal{L} , we notice that for the set $\{ZZI, IIX, ZII, IXX, ZZZ, XIX, IZI, XII, IZZ, XXX, ZIZ, IXI, IIZ, XXI\}$ of consecutive points of this graph (Fig. 2) the operators corresponding to neighboring points commute. Moreover, according to Table 1, after multiplying these commuting operators we get symmetric combinations (represented in Fig. 4 by the pink and orange circles) which again commute with their parents. In this way we obtain 28 points of symmetric combinations grouped into 14 lines, each containing three pairwise commuting operators such that the product of any two of them yields (up to a sign) the third one. It is therefore reasonable to regard this property as the basic one of incidence governing the structure of our representation of the Hexagon. One further sees that the 14 lines we have just described are of the point/line/flag type (e. g., the triple $\{XXI, ZZI, YYI\}$). These lines are called H1-lines [20], or lines of Coxeter type [27]. We have altogether 21 such lines (represented in Fig. 4 by dark grey arcs), with the remaining 7 of them connecting points related to commuting operators of point-line type to the remaining 7 symmetric operators (flags); these latter operators are

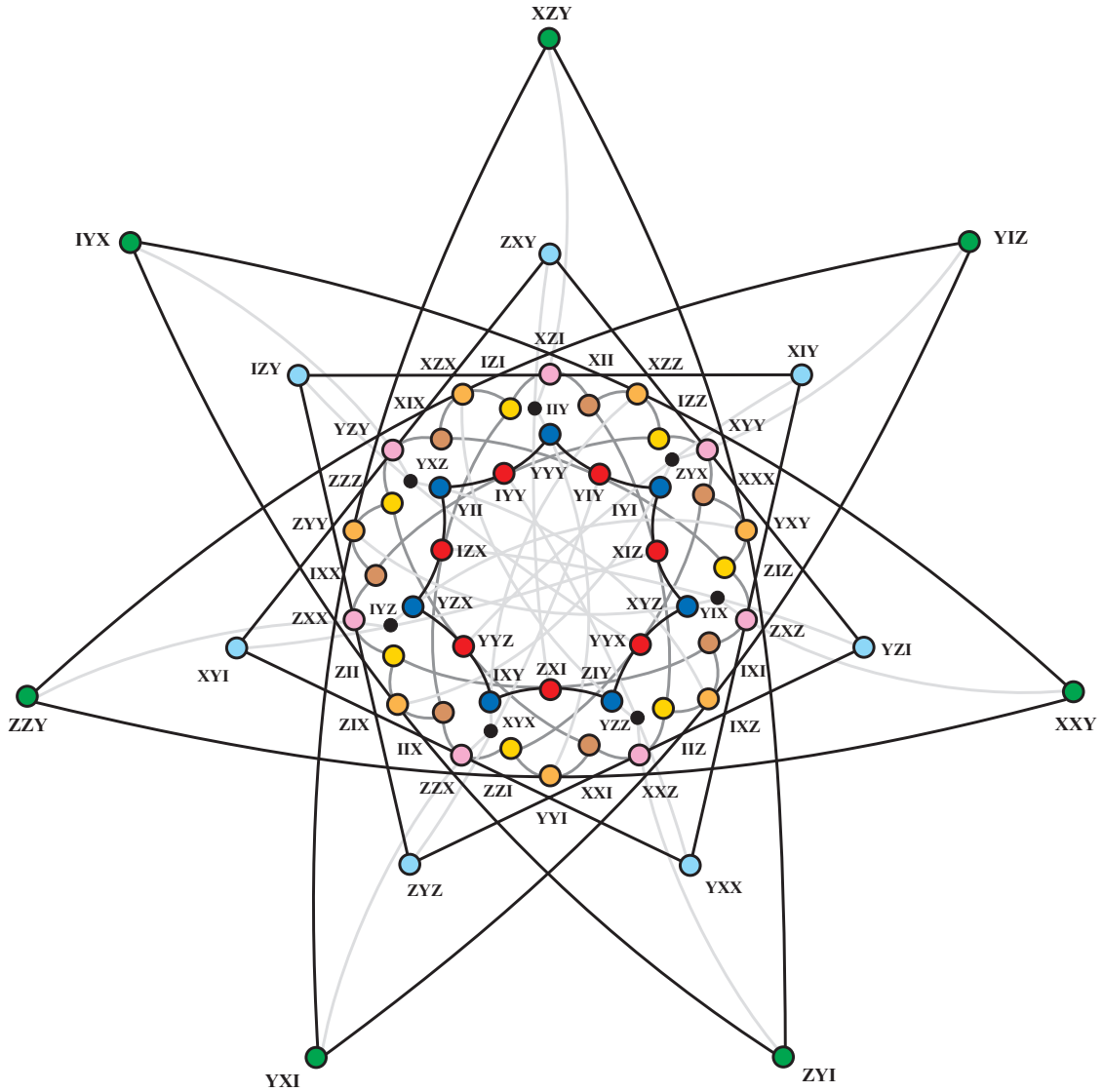


Figure 4: A diagrammatic illustration of the structure of the split Cayley hexagon of order two (after [18]–[20]) and how this geometry grasps the core features of the algebra of the real three-qubit Pauli matrices by bijectively associating the latter with the points of the hexagon. The points themselves are represented by circles whose interior is colored in nine different ways reflecting the nine orbits of an automorphism of order seven; the lines are drawn as black, light and dark grey curves/joints. The remaining symbols and notation are explained in the text.

represented by red circles in Fig. 4. Having employed the basic relations of incidence (*aka* up-to-a-sign multiplications producing triples of pairwise commuting operators), we have thus managed to establish the correspondence between 35 points of the Hexagon and 35 symmetric combinations on the one hand, and between 21 H1-lines and 21 triples of symmetric combinations on the other hand. As a consistency check, one readily sees that the order seven automorphism $\mathcal{D}(\alpha)$ rotates the operators corresponding to the yellow, brown, pink, orange and red points in the clockwise direction.

We still have to take care of the remaining 28 points (anti-flags) of the Hexagon that answer to antisymmetric combinations of operators, as well as for the remaining 42 H2-lines [20], also known as lines of Heawood type [27].¹ Let us deal first with the lines. These lines are of the flag/anti-flag/anti-flag type and their explicit construction is as follows. Take a (Fano) line L and a (Fano) point p lying on it. This gives rise to the flag $\{p, L\}$. Consider now the other two points q and r lying on the line L , and the other two lines M, N passing through the point p . Clearly, the two pairs $\{q, M\}, \{r, N\}$ and $\{q, N\}, \{r, M\}$ are two pairs of anti-flags. Hence, the flag $\{p, L\}$ gives rise to *two* H2-lines of the form $\{\{p, L\}, \{q, M\}, \{r, N\}\}$ and $\{\{p, L\}, \{q, N\}, \{r, M\}\}$. Since we have 21 flags the number of such lines is 42. In our representation in terms of operators of the Pauli group, these lines are represented by pairwise commuting triples containing two antisymmetric operators and a symmetric one with the property that any pair from the triple produces the remaining one under an up-to-a-sign multiplication. Given the representation of the Fano plane (Fig. 1, left, and Fig. 2) with its points labelled by the elements of the set \mathcal{P} and its lines by those from \mathcal{L} , it is a rather straightforward task to obtain all of these 42 triples, and to check our basic relations of incidence. As an illustrative example, one takes the point p represented by the operator ZII and the line L represented by the one IXX (see Fig. 1, left). From Table 1 one reads that they define the flag $\{p, L\}$ represented by the operator ZXX . The remaining two points on L are q and r represented by IZZ and ZZZ , respectively. The lines M and N going through p correspond, respectively, to the operators IIX and IXI . Hence, the operator representatives of the two pairs of anti-flags $\{q, M\}, \{r, N\}$ and $\{q, N\}, \{r, M\}$ are IZY, ZYZ and IYZ, ZZY , respectively. In this way we have obtained two H2-lines represented by the triples $\{ZXX, IZY, ZYZ\}$, and $\{ZXX, IYZ, ZZY\}$. The elements of these triples are pairwise commuting and the product of any two from a given triple indeed yields, up to a sign, the remaining one. Finally, we observe that exactly one half of these lines (represented by black arcs/segments in Fig. 4) enjoy the property of connecting two distinct points/operators from the same orbit.

When it comes to the remaining points of the Hexagon, all what we need is to make use of the special footing of the seven element set of antisymmetric matrices given by Eq. (17). For if we look at Fig. 4 carefully, the points (related to Fano anti-flags) represented by black bullets are also found to be special because the H2-lines passing through them (represented by light grey curves/arcs in Fig. 4) encompass not only all 21 points related to flags (red, pink and orange circles) but also all the remaining 21 points related to anti-flags (dark blue, light blue and green circles). None of the remaining points related to anti-flags exhibit this property. It is, therefore, natural to associate the points represented by black bullets with the matrices from \mathcal{L}' (Eq. (17)). Given this fact, and taking into account the structure of H2-lines, the seven-fold symmetry of the Hexagon and our up-to-a-sign multiplication recipe, after some experimenting we finally arrive at the full bijection between our real generalized three-qubit Pauli matrices and the points of the Hexagon as explicitly shown in Fig. 4.

To gain a fuller appreciation of the above-described geometrical picture of our operator algebra, we have to mention a very important representation of the Hexagon as a sub-geometry of $PG(5, 2)$, the five-dimensional projective space over the Galois field of two elements [18, 28, 29]. In this representation 63 points of the Hexagon coincide with 63 points of $PG(5, 2)$, 63 lines of the Hexagon form a special subset out of the total of 651 lines of $PG(5, 2)$, and the 35 points of the Hexagon associated with the *symmetric* combinations of the operators are nothing but the points of a *Klein quadric* in $PG(5, 2)$. And as there exists

¹The names of the two types of lines are dictated by the fact that after removing the points of flag type from the Hexagon we are left with two connected graphs — the Heawood graph and the Coxeter graph (see below); the edges of the former/latter corresponding to the lines of Heawood/Coxeter type.

a bijection between this special set of points of $PG(5, 2)$ and the 35 lines of $PG(3, 2)$, which completely encodes this projective three-space (see, e. g., [30]), properties of our symmetric combinations are thus seen to be also embodied in the configuration of the lines of this smallest projective space.

We shall conclude this section with the following important observation. Let us pick up one point represented by a black bullet. This point is associated with a unique set of seven points (including the point itself) which are located on the three lines passing through the point in question. In terms of our bijection, we thus have seven (one per each black bullet) distinguished sets of operators, viz.

$$\mathcal{B}_1 = \{YZZ, XXZ, ZYI, YXX, IYY, ZIY, XZX\}, \quad (23)$$

$$\mathcal{B}_2 = \{YIX, ZXZ, XXY, YZI, IZX, XYZ, ZYY\}, \quad (24)$$

$$\mathcal{B}_3 = \{ZYX, XYY, YIZ, XIY, YYZ, IYI, ZIX\}, \quad (25)$$

$$\mathcal{B}_4 = \{IIY, XZI, XZY, ZXY, ZXI, YYY, YYI\}, \quad (26)$$

$$\mathcal{B}_5 = \{YXZ, YZY, IYX, IZY, YYX, YII, IXZ\}, \quad (27)$$

$$\mathcal{B}_6 = \{IYZ, ZXX, ZZY, XYI, XIZ, YZX, YXY\}, \quad (28)$$

$$\mathcal{B}_7 = \{XYX, ZZX, YXI, ZYZ, YIY, IXY, XZZ\}. \quad (29)$$

Let us add to this list the two sets \mathcal{P} and \mathcal{L} , renamed as

$$\mathcal{B}_8 = \mathcal{P}, \quad \mathcal{B}_9 = \mathcal{L}. \quad (30)$$

After lengthy, yet straightforward, calculations one can verify that each of them consists of pairwise commuting operators and when taken together they give rise to a maximum ($d + 1 = 8 + 1 = 9$) set of mutually unbiased bases (MUBs) in this particular three-qubit Hilbert space.

5 The subgroup $PSL_2(7)$ of the full automorphism group of the Hexagon

The Hexagon has a high degree of symmetry. By a symmetry we mean a bijection sending points to points such that this transformation induces a bijection between the line sets as well. We have already encountered the seven-fold symmetry of the Hexagon related to the permutation α and its 8×8 matrix representation $\mathcal{D}(\alpha)$ of Eq. (10). It is known that the full symmetry group of the Hexagon is of order 12096, being basically isomorphic to the Chevalley group $G_2(2)$ [19, 21]. In this paper, however, we are merely interested in an important subgroup of the full automorphism group of the Hexagon realized on three qubits. This subgroup, which is directly related to the one of the Fano plane, is Klein's group $PSL_2(7)$ of order 168. In the following section, a 8×8 representation of this subgroup on three qubits will play an important role in illustrating how the geometry of the Hexagon manifests itself in the physics of certain stringy black hole solutions.

The presentation of $PSL_2(7)$ we have found convenient [31] is that based on three generators α, β and γ

$$PSL_2(7) \equiv \{\alpha, \beta, \gamma \mid \alpha^7 = \beta^3 = \gamma^2 = \alpha^{-2}\beta\alpha\beta^{-1} = (\gamma\beta)^2 = (\gamma\alpha)^3 = 1\}. \quad (31)$$

In the following two possible ways of realizing $PSL_2(7)$ in terms of permutations of the symbols $1, 2, \dots, 7$ will be needed. They are

$$\alpha \equiv (1234567), \quad \beta \equiv (124)(365)(7), \quad \gamma \equiv (12)(36)(4)(5)(7), \quad (32)$$

and

$$\alpha' \equiv (1234567), \quad \beta' \equiv (1)(235)(476), \quad \gamma' \equiv (1)(3)(4)(25)(67). \quad (33)$$

Our convention for multiplying permutations is from right to left (i. e., opposite to that adopted in Conway and Sloane [31]). One can check that the generators α, β, γ and α', β', γ' satisfy the defining relations of Eq. (31). An important observation is that if we permute the points of the Fano plane by $PSL_2(7)$ transformations generated by the set α, β, γ then this implies a permutation on the lines generated by the elements α', β', γ' . Hence, the set defined by Eq. (32) generates transformations for the points of the Fano plane and the set of Eq. (33) for the points of its dual (see Fig. 1).

What we need is an 8×8 representation of $PSL_2(7)$ acting on three-qubits. It is clear that the 8×8 dimensional representation we are looking for is the one for which α is represented by $\mathcal{D}(\alpha)$ of Eq. (10). For the remaining generators, we have found the following representatives

$$\mathcal{D}(\beta) = C_{12}C_{21} = \begin{pmatrix} I & 0 & 0 & 0 \\ 0 & 0 & 0 & I \\ 0 & I & 0 & 0 \\ 0 & 0 & I & 0 \end{pmatrix}, \quad (34)$$

$$\mathcal{D}(\gamma) = C_{21}(I \otimes I \otimes Z) = \begin{pmatrix} Z & 0 & 0 & 0 \\ 0 & 0 & 0 & Z \\ 0 & 0 & Z & 0 \\ 0 & Z & 0 & 0 \end{pmatrix}, \quad (35)$$

with the CNOT operations defined by Eq. (19). It is straightforward to check that $\mathcal{D}(\alpha), \mathcal{D}(\beta)$ and $\mathcal{D}(\gamma)$ all satisfy the defining relations of Eq. (31). It is important to realize that in this way we managed to realize Klein's group $PSL_2(7)$ on three qubits in terms of CNOT operations and a single "phase gate" Z . (The "phase" change in this case is just a sign change in the third qubit.) Hence, Klein's group operates quite naturally on the set $\mathcal{M} \equiv \{\pm I, \pm X, \pm Y, \pm Z\}$ of the real operators of the Pauli group.

Since the order seven automorphism $\mathcal{D}(\alpha)$ is by its very construction a symmetry, in order to demonstrate the $PSL_2(7)$ symmetry of the Hexagon we have to check the action of the remaining generators $\mathcal{D}(\beta)$ and $\mathcal{D}(\gamma)$ on the three-qubit operators associated with the points of the Hexagon. To this end, it is convenient to replace our original labelling scheme (which was motivated by and based on the Polster and his co-workers' labelling of the points and lines of the Hexagon [18]–[20]) by the one shown in Table 2. So, for example, the set $\{g_k \mid k = 1, 2, \dots, 7\}$ corresponds to our set \mathcal{L}' of operators of Eq. (17) playing a special role (black bullets in Fig. 4) and the lines of the Hexagon can be written in a nice compact notation as follows

$$A_k = \{g_{k+1}, c_{k+3}, a_{k+4}\}, B_k = \{f_{k-2}, b_k, g_{k+1}\}, D_k = \{d_{k-1}, g_{k+1}, e_{k+2}\}, \quad (36)$$

$$C_k = \{c_{k-2}, b_k, c_{k+1}\}, E_k = \{e_{k+1}, e_{k+3}, a_{k+4}\}, F_k = \{d_{k-1}, f_{k+1}, f_{k+2}\}, \quad (37)$$

Table 2: The matrix products between the generalized Pauli operators from the two distinguished sets in terms of the new labelling scheme (compare with Table 1).

L/P	h_1	h_2	h_3	h_4	h_5	h_6	h_7
i_1	a_1	b_1	c_1	d_1	e_1	f_1	g_1
i_2	g_2	a_2	b_2	c_2	d_2	e_2	f_2
i_3	f_3	g_3	a_3	b_3	c_3	d_3	e_3
i_4	e_4	f_4	g_4	a_4	b_4	c_4	d_4
i_5	d_5	e_5	f_5	g_5	a_5	b_5	c_5
i_6	c_6	d_6	e_6	f_6	g_6	a_6	b_6
i_7	b_7	c_7	d_7	e_7	f_7	g_7	a_7

$$G_k = \{d_{k-1}, h_{k+2}, i_{k-1}\}, H_k = \{a_{k+4}, h_{k+4}, i_{k+4}\}, I_k = \{b_k, h_{k+1}, i_k\}. \quad (38)$$

Just to familiarize ourselves with this new notation, we pick up one line of the Hexagon, say $C_1 = \{c_6, b_1, c_2\}$. According to Tables 1–2, this line is an H2-line of the form $\{ZYI, ZIX, IYX\}$ depicted in Fig. 4 by the colour combination green-orange-green. In a similar way one finds that the line $G_3 = \{d_2, h_5, i_2\} = \{IYY, IZZ, IXX\}$, with the colour combination red-yellow-brown, is an H1-line. Obviously, the 42 lines of type A, B, C, D, E, F are H2-lines, and the 21 ones of G, H, I type are H1-lines. The lines containing the special set \mathcal{L}' are the ones of A, B, D ; As already remarked in the previous section, (operators located on) these lines (represented in Fig. 4 by light grey acrs) give rise to a maximum set of MUBS.

Let us demonstrate the $PSL_2(7)$ symmetry of the Hexagon. Since we have already proved its seven-fold symmetry, we only have to check how the generators $\mathcal{D}(\beta)$ and $\mathcal{D}(\gamma)$ act on the points and lines of the Hexagon. Let us consider first the action of $\mathcal{D}(\beta)$. We introduce the notation

$$(rst)_{ijk} \equiv (r_i s_j t_k)(s_i t_j r_k)(t_i r_j s_k), \quad (rst)_i \equiv (r_i s_i t_i), \quad i, j, k = 1, 2, \dots, 7, \quad (39)$$

where (rst) , as usual, refers to the cyclic permutation of the symbols rst . More generally, we can consider expressions like

$$(rst)(uvw)_{(ijk)(lmn)(p)} \equiv (rst)_{ijk}(rst)_{lmn}(rst)_p(uvw)_{ijk}(uvw)_{lmn}(uvw)_p \quad (40)$$

where $(ijk)(lmn)(p)$ is a permutation of the ordered set $\{1, 2, \dots, 7\}$ in a cycle notation. Terms like $(r)_{ijk}$ have no meaning hence they are not included. Thus, for example, $(uvw)(r)_{(ijk)(l)}$ stands for $(uvw)_{ijk}(uvw)_l r_l$. The action of $\mathcal{D}(\beta)$ on the points and lines of the Hexagon is thus given by

$$(adb)(cef)(g)(i)_{(1)(253)(467)}, \quad (h)_{(142)(356)(7)}, \quad (41)$$

and

$$(ADB)(CEF)(GIH)_{(142)(356)(7)}, \quad (42)$$

respectively. Notice that this action is tied to the *inverse* of the basic permutations β and β' of Eqs. (32)–(33) related to the corresponding action on the sets $\mathcal{P}(\{h_k \mid k = 1, 2, \dots, 7\})$ and $\mathcal{L}(\{i_k \mid k = 1, 2, \dots, 7\})$ labelling the points and lines of the Fano plane.

Let us now look at the action of $\mathcal{D}(\gamma)$. A straightforward calculation shows that the points transform in the following way

$$(a_1 b_1)(d_1)(c_1 f_1)(e_1)(g_1), \quad (a_3 d_3)(b_3)(c_3)(e_3)(f_3 g_3), \quad (43)$$

$$(a_2d_5)(d_2a_5)(b_2b_5)(c_2g_5)(g_2e_5)(e_2f_5)(f_2c_5), \quad (44)$$

$$(a_4)(b_4)(d_4)(c_4g_4)(e_4f_4), \quad (a_6d_7)(d_6b_7)(b_6a_7)(c_6c_7)(e_6g_7)(g_6f_7)(f_6e_7), \quad (45)$$

$$(h_1h_2)(h_3h_6)(h_4)(h_5)(h_7), \quad (i_1)(i_2i_5)(i_3)(i_4)(i_6i_7). \quad (46)$$

It is important to stress here that the quantities in Eqs. (43)–(44), as well as i_1, i_2, i_3 , and i_5 , transform with a sign change; thus, for example, (a_1b_1) and (i_1) refer to the transformations $a_1 \leftrightarrow -b_1$ and $i_1 \leftrightarrow -i_1$. However, since our labelling of the points of the Hexagon by the real Pauli operators is only *up to a sign*, this additional action of the group \mathbf{Z}_2 is not of current interest for us. Notice that the transformation rules given by Eqs. (43)–(45), as well as of those of the points $\{i_k\}$, can be expressed by the permutations of the form (1)(3)(25)(4)(67), which is just γ' of Eq. (33). Moreover, the transformation property $(ab)(d)(cf)(e)(g)$ of Eq. (43) and the one of the points $\{h_k\}$ is associated with (12)(4)(36)(5)(7), i. e., with the permutation γ of Eq. (32). Of course, the transformations on the sets $\{i_k\}$ and $\{h_k\}$ are again the ordinary ones of the points and lines of the Fano plane.

Finally, we verify that the action of $\mathcal{D}(\gamma)$ on the points also induces a bijection on the lines, which is of the form

$$(A_1D_3)(A_2F_1)(A_3C_6)(A_4C_1)(A_5F_6)(A_6D_4)(A_7), \quad (47)$$

$$(B_1E_4)(B_2B_5)(B_3C_3)(B_4C_4)(B_6E_3)(B_7D_7)(C_2C_5)(C_7F_7), \quad (48)$$

$$(D_1E_2)(D_2F_2)(D_5F_5)(D_6E_5)(E_1F_3)(E_6F_4)(E_7), \quad (49)$$

$$(G_1H_2)(G_2)(G_3H_1)(G_4H_6)(G_5)(G_6H_5)(G_7I_7), \quad (50)$$

$$(H_3I_6)(H_4I_1)(H_7)(I_2I_5)(I_3)(I_4). \quad (51)$$

We see that under both $\mathcal{D}(\beta)$ and $\mathcal{D}(\gamma)$ the sets of H1- and H2-lines are left invariant. Hence, the $PSL_2(7)$ subgroup of the full automorphism group of the Hexagon preserves the splitting of its lines into these two subclasses. The same is also true for the two distinguished subsets of points. This is a very important finding which tells us that this subgroup also preserves the sub-configuration of the Hexagon formed by its 28 anti-flag points and 42 H2-lines which is isomorphic — as depicted in Fig. 5 — to the famous Coxeter graph [32], the second of the two remarkable graphs living in the Hexagon (see also [20]). We shall make use of this result in the next section. For the sake of completeness, we here only add that the Hexagon contains 36 different copies of the Coxeter graph and the same number of copies of the Heawood graph as well.

6 Coxeter sub-geometry and $E_{7(7)}$ -symmetric black hole solutions

In this section we would like to show how the Coxeter sub-geometry of the Hexagon manifests itself in the geometry of a certain class of stringy black hole solutions. In string theory it

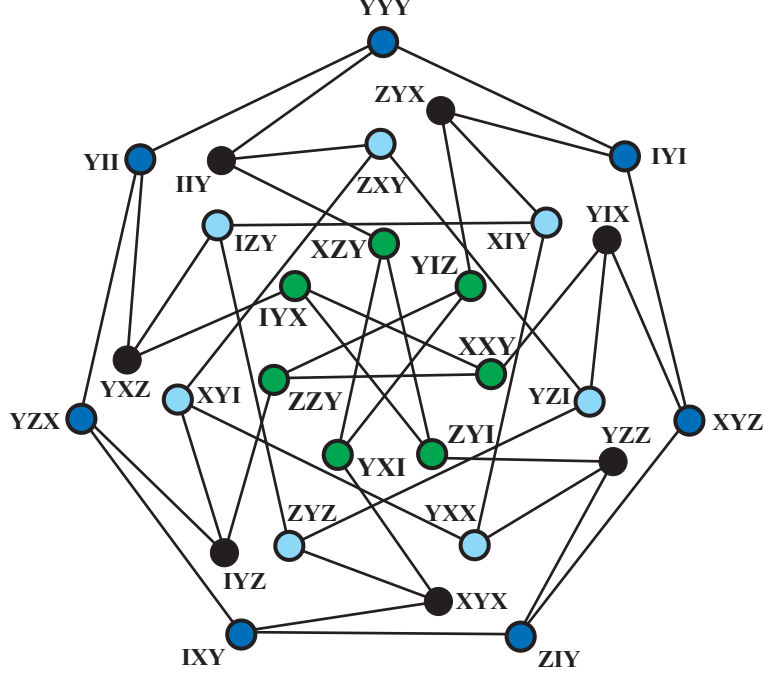


Figure 5: The Coxeter graph, in a form showing its automorphism of order seven, as a subgraph/subgeometry of the Hexagon (see Fig. 4).

is well known that the most general class of black hole solutions in $N = 8$ supergravity/M-theory in four dimensions is defined by 56 charges (28 electric and 28 magnetic), and the entropy formula for such solutions is related to the square root of the quartic Cartan-Cremmer-Julia $E_{7(7)}$ invariant [33]–[36]

$$S = \pi \sqrt{|J_4|}. \quad (52)$$

Here, the Cremmer-Julia form of this invariant [36] depends on the antisymmetric complex 8×8 central charge matrix \mathcal{Z} ,

$$J_4 = \text{Tr}(\mathcal{Z}\overline{\mathcal{Z}})^2 - \frac{1}{4}(\text{Tr}\mathcal{Z}\overline{\mathcal{Z}})^2 + 4(\text{Pf}\mathcal{Z} + \text{Pf}\overline{\mathcal{Z}}), \quad (53)$$

where the overbars refer to complex conjugation. The definition of the Pfaffian is

$$\text{Pf}\mathcal{Z} = \frac{1}{2^4 \cdot 4!} \epsilon^{ABCDEFGH} \mathcal{Z}_{AB} \mathcal{Z}_{CD} \mathcal{Z}_{EF} \mathcal{Z}_{GH}. \quad (54)$$

An alternative form of this invariant is the one given by Cartan [34]

$$J_4 = -\text{Tr}(xy)^2 + \frac{1}{4}(\text{Tr}xy)^2 - 4(\text{Pf}x + \text{Pf}y). \quad (55)$$

Here, the 8×8 matrices x and y are antisymmetric ones containing 28 electric and 28 magnetic charges which are integers due to quantization. These charges are related to some numbers of membranes wrapping around the extra dimensions these objects live in [35]. The relation between the Cremmer-Julia and Cartan forms has been established [37] by using the relation

$$\mathcal{Z}_{AB} = -\frac{1}{4\sqrt{2}}(x^{IJ} + iy_{IJ})(\Gamma^{IJ})_{AB}, \quad (56)$$

where summation through the indices I, J is implied. Here $(\Gamma^{IJ})_{AB}$ are the generators of the $SO(8)$ algebra, where (IJ) are the vector indices ($I, J = 0, 1, \dots, 7$) and (AB) are the

spinor ones ($A, B = 0, 1, \dots, 7$). Triality of $SO(8)$ ensures that we can transform between its vector and spinor representations. A consequence of this is that we can also invert the relation of Eq. (56) and express $x^{IJ} + iy_{IJ}$ in terms of the matrix of central charge \mathcal{Z}_{AB} .

Since the matrices $x^{IJ} + iy_{IJ}$ and \mathcal{Z}_{AB} are both 8×8 antisymmetric ones with 28 independent components, it is natural to expect that the Coxeter sub-geometry of the Hexagon should provide additional insight into the structure of the $E_{7(7)}$ symmetric black hole entropy formula. In order to see that this is indeed the case, all we have to do is to recall from Sec. 3 that the elements of our distinguished set \mathcal{L}' of Eq. (17), corresponding to the points of the Hexagon represented by black bullets (see Fig. 4), are related to a seven dimensional Clifford algebra. Moreover, commutators of the form $[\Gamma_j, \Gamma_k]$, $j, k = 1, 2, \dots, 7$, give rise to the 21 generators of an $SO(7)$ subalgebra. Hence, the 28 antisymmetric matrices $(\Gamma^{IJ})_{AB}$ occurring in Eq. (56) should be related to the 28 ones of the Coxeter set (see Eqs. (14)–(17) and Fig. 5). A natural choice for relating these two sets is

$$\{g_k\} \leftrightarrow \Gamma^{0k}, \quad [g_j, g_k] \leftrightarrow \Gamma^{jk}. \quad (57)$$

According to our labelling scheme of Table 2, we see that the 28 $SO(8)$ generators $(\Gamma^{IJ})_{AB}$ are divided into the four sets $\{g_k\}$, $\{b_k\}$, $\{e_k\}$ and $\{f_k\}$, $k = 1, 2, \dots, 7$. An explicit relation between these quantities is

$$-\Gamma^{IJ} = \begin{pmatrix} 0 & g_1 & g_2 & g_3 & g_4 & g_5 & g_6 & g_7 \\ -g_1 & 0 & e_6 & c_4 & -f_3 & f_7 & -c_2 & -e_5 \\ -g_2 & -e_6 & 0 & e_7 & c_5 & -f_4 & f_1 & -c_3 \\ -g_3 & -c_4 & -e_7 & 0 & e_1 & c_6 & -f_5 & f_2 \\ -g_4 & f_3 & -c_5 & -e_1 & 0 & e_2 & c_7 & -f_6 \\ -g_5 & -f_7 & f_4 & -c_6 & -e_2 & 0 & e_3 & c_1 \\ -g_6 & c_2 & -f_1 & f_5 & -c_7 & -e_3 & 0 & e_4 \\ -g_7 & e_5 & c_3 & -f_2 & f_6 & -c_1 & -e_4 & 0 \end{pmatrix}. \quad (58)$$

Here, the first row and column corresponding to the entries Γ^{0k} and Γ^{k0} are related to the special set $\{g_k\}$. The entries of the remaining 7×7 block are given by the formula $\frac{1}{2}[g_j, g_k]$. Thus, for example, according to Tables 1 and 2 we have $-\Gamma^{25} = \frac{1}{2}[g_2, g_5] = \frac{1}{2}[ZYX, XYX] = -YII = -f_4$. (All the entries of this matrix Γ^{IJ} are 8×8 matrices, hence the spinor indices AB are left implicit.)

An important consequence of this explicit correspondence is that the 28 Gaussian integers (regarded as expansion coefficients for \mathcal{Z}) comprising the antisymmetric charge matrix $x^{IJ} + iy_{IJ}$ can also be divided into seven sets. This division answers to the similar one of the ‘‘basis’’ vectors $\{g_k, e_k, c_k, f_k\}$, $k = 1, 2, \dots, 7$, corresponding to Γ^{IJ} . For historical reasons (to be explained below) we chose the *dual labelling* for the elements of the charge matrix $x^{IJ} + iy_{IJ}$

$$x^{IJ} = \begin{pmatrix} 0 & -\mathbf{a}_7 & -\mathbf{b}_7 & -\mathbf{c}_7 & -\mathbf{d}_7 & -\mathbf{e}_7 & -\mathbf{f}_7 & -\mathbf{g}_7 \\ \mathbf{a}_7 & 0 & \mathbf{f}_1 & \mathbf{d}_4 & -\mathbf{c}_2 & \mathbf{g}_2 & -\mathbf{b}_4 & -\mathbf{e}_1 \\ \mathbf{b}_7 & -\mathbf{f}_1 & 0 & \mathbf{g}_1 & \mathbf{e}_4 & -\mathbf{d}_2 & \mathbf{a}_2 & -\mathbf{c}_4 \\ \mathbf{c}_7 & -\mathbf{d}_4 & -\mathbf{g}_1 & 0 & \mathbf{a}_1 & \mathbf{f}_4 & -\mathbf{e}_2 & \mathbf{b}_2 \\ \mathbf{d}_7 & \mathbf{c}_2 & -\mathbf{e}_4 & -\mathbf{a}_1 & 0 & \mathbf{b}_1 & \mathbf{g}_4 & -\mathbf{f}_2 \\ \mathbf{e}_7 & -\mathbf{g}_2 & \mathbf{d}_2 & -\mathbf{f}_4 & -\mathbf{b}_1 & 0 & \mathbf{c}_1 & \mathbf{a}_4 \\ \mathbf{f}_7 & \mathbf{b}_4 & -\mathbf{a}_2 & \mathbf{e}_2 & -\mathbf{g}_4 & -\mathbf{c}_1 & 0 & \mathbf{d}_1 \\ \mathbf{g}_7 & \mathbf{e}_1 & \mathbf{c}_4 & -\mathbf{b}_2 & \mathbf{f}_2 & -\mathbf{a}_4 & -\mathbf{d}_1 & 0 \end{pmatrix}, \quad (59)$$

$$y_{IJ} = \begin{pmatrix} 0 & -\mathbf{a}_0 & -\mathbf{b}_0 & -\mathbf{c}_0 & -\mathbf{d}_0 & -\mathbf{e}_0 & -\mathbf{f}_0 & -\mathbf{g}_0 \\ \mathbf{a}_0 & 0 & \mathbf{f}_6 & \mathbf{d}_3 & -\mathbf{c}_5 & \mathbf{g}_5 & -\mathbf{b}_3 & -\mathbf{e}_6 \\ \mathbf{b}_0 & -\mathbf{f}_6 & 0 & \mathbf{g}_6 & \mathbf{e}_3 & -\mathbf{d}_5 & \mathbf{a}_5 & -\mathbf{c}_3 \\ \mathbf{c}_0 & -\mathbf{d}_3 & -\mathbf{g}_6 & 0 & \mathbf{a}_6 & \mathbf{f}_3 & -\mathbf{e}_5 & \mathbf{b}_5 \\ \mathbf{d}_0 & \mathbf{c}_5 & -\mathbf{e}_3 & -\mathbf{a}_6 & 0 & \mathbf{b}_6 & \mathbf{g}_3 & -\mathbf{f}_5 \\ \mathbf{e}_0 & -\mathbf{g}_5 & \mathbf{d}_5 & -\mathbf{f}_3 & -\mathbf{b}_6 & 0 & \mathbf{c}_6 & \mathbf{a}_3 \\ \mathbf{f}_0 & \mathbf{b}_3 & -\mathbf{a}_5 & \mathbf{e}_5 & -\mathbf{g}_3 & -\mathbf{c}_6 & 0 & \mathbf{d}_6 \\ \mathbf{g}_0 & \mathbf{e}_6 & \mathbf{c}_3 & -\mathbf{b}_5 & \mathbf{f}_5 & -\mathbf{a}_3 & -\mathbf{d}_6 & 0 \end{pmatrix}. \quad (60)$$

Here, we used boldface letters for the coefficients $\mathbf{a}_J, \dots, \mathbf{g}_J, J = 0, 1, \dots, 7$, not to be confused with the letters $a_j, \dots, g_j, j = 1, 2, \dots, 7$, denoting 8×8 matrices. This labelling can be summarized as

$$\{1, 2, 3, 4, 5, 6, 7\} \leftrightarrow \{\mathbf{a}, \mathbf{b}, \mathbf{c}, \mathbf{d}, \mathbf{e}, \mathbf{f}, \mathbf{g}\} \quad (61)$$

$$\{g, e, , c, f\} \leftrightarrow \{70, 16, 43, 25\}. \quad (62)$$

The symbols on the left-hand side of Eqs. (61)–(62) label the basis vectors, those on the right hand side the expansion coefficients of the central charge matrix \mathcal{Z} . In other words, we are converting numbers occurring in the sets $\{g_k, e_k, c_k, f_k\}, k = 1, \dots, 7$, to boldface letters in a lexicographic order and the letters g, e, c, f to numbers according to the rule of Eq. (62). This means that, for example, we use the notation for the expansion coefficient $x^{36} + iy_{36}$ attaching to the “basis vector” $-\Gamma^{36} \sim -f_5$ the symbol $-\mathbf{e}_2 - i\mathbf{e}_5$; that is, 5 was converted to \mathbf{e} and the letter f was converted to the numbers 2 and 5 corresponding to the real and imaginary parts of the charge matrix.

In this way we can associate the 28 points of the Coxeter sub-geometry of the Hexagon to 28 Gaussian integers with the real and imaginary parts corresponding to electric and magnetic charges characterizing the particular charge configuration of the black hole solution. Explicitly, according to Tables 1 and 2, the sets of points represented by the (black, green, light blue, dark blue) circles in Fig. 5 can be associated with the “basis vectors” $(g_k, c_k, e_k, f_k), k = 1, 2, \dots, 7$. Moreover, according to Eqs. (58)–(60), with these “basis vectors” we can associate the corresponding “expansion coefficients,” i. e., the charge combinations.

By virtue of the seven-fold symmetry of the Coxeter graph we also have managed to divide the 56 charges characterizing the particular black hole solution into 7 subsets with 8 elements each. It can be shown [4, 5] that each of these 7 sets can be regarded as 7 three-qubit states with the 8 elements being their integer-valued amplitudes. The explicit dictionary in the form of Eqs. (59) and (60) between the amplitudes of these three-qubit states and the elements of the charge matrices x^{IJ} and y_{IJ} were first obtained by Duff and his co-workers [38]. Here, we recovered this result by a straightforward way from the geometry of the Hexagon. It was also shown [4, 5] that the transformation properties of the 56 charges related to such three-qubit states under the fundamental representation of the exceptional group E_7 can be described by introducing an entangled state of seven qubits related to the geometry of the Fano plane. This seven-qubit system, however, contains merely tripartite entanglement in the form of our seven three-qubit systems we have just found.

Notice that our present approach to this unusual type of entanglement is *fundamentally* different from those based on seven qubits. Here we managed to describe the charge configurations of black hole solutions by using the algebra of *observables* on *three*-qubits. By comparison in these recent approaches such configurations have been described by special *states* on *seven*-qubits forming a 56 dimensional subspace of the state space of *seven qutrits* [4].

In the previous section we have shown that the Coxeter sub-geometry has a $PSL_2(7)$ symmetry. Due to the relationship found between this geometry and the charge configurations we expect that this symmetry should also manifest itself in the black hole entropy formula. That this should be the case is already known from the mathematical literature [39]. However, now we can demonstrate this symmetry quite easily. Recall our 8×8 matrix representation of $PSL_2(7)$ generated by the matrices $\mathcal{D}(\alpha), \mathcal{D}(\beta), \mathcal{D}(\gamma)$. It is easy to check that these generators are elements of the group $SO(8)$. Since under an element $O \in SO(8)$ the Pfaffian transforms as $\text{Pf}(OZO^t) = (\text{Det}O)\text{Pf}(\mathcal{Z}) = \text{Pf}(\mathcal{Z})$, from Eq. (53) one can immediately check that J_4 , and so the black hole entropy formula, is invariant under $PSL_2(7)$. This should not come as a surprise since each of the terms of Eq. (53) has manifest $SU(8)$ symmetry and all of our generators can be embedded into this subgroup of $E_{7(7)}$. What is not trivial, however, is the explicit form of this $PSL_2(7)$ action on the charge matrix

$x^{IJ} + iy_{IJ}$ which is simply the one induced by a similar action of conjugation on the basis vectors Γ^{IJ} . This explicit action on the ‘‘basis vectors’’ $\{g_k, c_k, e_k, f_k\}, k = 1, \dots, 7$, related to Γ^{IJ} via Eq. (58), is

$$\mathcal{D}(\alpha) : (c)(e)(f)(g)_{(1234567)}, \quad (63)$$

$$\mathcal{D}(\beta) : (cef)(g)_{(1)(253)(457)}, \quad (64)$$

$$\mathcal{D}(\gamma) : (c_1 f_1)(e_1)(g_1), \quad (c_2 g_5)(g_2 e_5)(e_2 f_5)(f_2 c_5), \quad (c_3)(e_3)(f_3 g_3), \quad (65)$$

$$\mathcal{D}(\gamma) : (c_4 g_4)(e_4 f_4), \quad (c_6 c_7)(e_6 g_7)(g_6 f_7)(f_6 e_7). \quad (66)$$

Here, we again note that the quantities of Eq. (65) transform with a sign change, i. e., $(c_1 f_1)$ means $c_1 \leftrightarrow -f_1$ (see Eqs. (41),(43)–(45)). By virtue of the correspondence as given by Eqs. (56),(58)–(60), it is easy to obtain the corresponding explicit $PSL_2(7)$ action on the charge matrices x and y , or, alternatively, on the seven three-qubit systems built from seven qubits [4, 5]. This explicit action of the $PSL_2(7)$ symmetry can be regarded as a subgroup of transformations of the full U -duality group $E_7(\mathbf{Z})$. Notice also that we have managed to represent this duality subgroup in terms of three-qubit CNOT operations creating and destroying entanglement and a trivial phase gate Z .

As the last application of the Coxeter sub-geometry to stringy black hole solutions, let us consider the canonical form of the central charge matrix \mathcal{Z} . As it is well known, by a transformation of the form $\mathcal{Z} \mapsto U^t \mathcal{Z} U$, where $U \in SU(8)$, \mathcal{Z} can be brought into the form

$$\mathcal{Z}_{\text{canonical}} = \begin{pmatrix} z_1 & 0 & 0 & 0 \\ 0 & z_1 & 0 & 0 \\ 0 & 0 & z_3 & 0 \\ 0 & 0 & 0 & z_4 \end{pmatrix} \otimes Y, \quad (67)$$

where all four z_j could be chosen to have the same phase, or three of the z_i could be chosen to be real [35]. Observing that the antisymmetric combinations c_1, e_1, f_1, g_1 occurring in the first row of Table 1 have the following explicit forms

$$c_1 = \begin{pmatrix} 1 & 0 & 0 & 0 \\ 0 & -1 & 0 & 0 \\ 0 & 0 & -1 & 0 \\ 0 & 0 & 0 & 1 \end{pmatrix} \otimes Y, \quad e_1 = \begin{pmatrix} 1 & 0 & 0 & 0 \\ 0 & -1 & 0 & 0 \\ 0 & 0 & 1 & 0 \\ 0 & 0 & 0 & -1 \end{pmatrix} \otimes Y, \quad (68)$$

$$f_1 = \begin{pmatrix} 1 & 0 & 0 & 0 \\ 0 & 1 & 0 & 0 \\ 0 & 0 & -1 & 0 \\ 0 & 0 & 0 & -1 \end{pmatrix} \otimes Y, \quad g_1 = \begin{pmatrix} 1 & 0 & 0 & 0 \\ 0 & 1 & 0 & 0 \\ 0 & 0 & 1 & 0 \\ 0 & 0 & 0 & 1 \end{pmatrix} \otimes Y, \quad (69)$$

we see that obtaining the canonical form corresponds to the situation of attaching charges merely to the points of the Coxeter graph labelled by ZZY, IZY, ZIY and IIY (see Fig. 5).

Let us first assume that the numbers z_i are all real. Then, employing Eqs. (56),(58) and (59), we get

$$\sqrt{8}\mathcal{Z} = x^{01}g_1 + x^{34}e_1 + x^{57}c_1 + x^{26}f_1 = -\mathbf{a}_7 g_1 + \mathbf{a}_1 e_1 + \mathbf{a}_4 c_1 + \mathbf{a}_2 f_1. \quad (70)$$

Hence, in this case we have

$$z_1 = \frac{1}{\sqrt{8}}(-\mathbf{a}_7 + \mathbf{a}_2 + \mathbf{a}_1 + \mathbf{a}_4), \quad z_2 = \frac{1}{\sqrt{8}}(-\mathbf{a}_7 + \mathbf{a}_2 - \mathbf{a}_1 - \mathbf{a}_4), \quad (71)$$

$$z_3 = \frac{1}{\sqrt{8}}(-\mathbf{a}_7 - \mathbf{a}_2 + \mathbf{a}_1 - \mathbf{a}_4), \quad z_4 = \frac{1}{\sqrt{8}}(-\mathbf{a}_7 - \mathbf{a}_2 - \mathbf{a}_1 + \mathbf{a}_4), \quad (72)$$

with the entropy formula

$$S = \pi \sqrt{|-4\mathbf{a}_1\mathbf{a}_2\mathbf{a}_4\mathbf{a}_7|} \quad (73)$$

being just the usual one obtained for four-charge extremal black holes [35]. (We remind that J_4 is positive for BPS and negative for non-BPS charge combinations.)

In the usual “tripartite-entanglement-of-seven-qubits” interpretation [4, 5] of the fundamental representation of E_7 we have seven three-qubit states with amplitudes $\mathbf{a}_I, \dots, \mathbf{g}_I, I = 0, 1, \dots, 7$. In this picture, obtaining the canonical form is simply restriction to just one of such three-qubit states (in this case to the one with amplitudes \mathbf{a}_I). This process is equivalent to the one with $-\mathbf{a}_7 - i\mathbf{a}_0$ attached to the black circle labelled by IIY , and $\mathbf{a}_4 + i\mathbf{a}_3$, $\mathbf{a}_2 + i\mathbf{a}_5$ and $\mathbf{a}_1 + i\mathbf{a}_6$ to the circles labelled by ZZY , ZIY and IZY , i. e., to the corresponding green, dark blue and light blue elements of Fig. 5. As explained elsewhere [2, 4, 5], the black hole entropy formula in this case is related to Cayley’s hyperdeterminant [1], i. e., to the unique triality and $SL(2)^{\otimes 3}$ invariant entanglement measure for three qubits. Indeed, a straightforward calculation in this case shows that $J_4 = -D(\mathbf{a})$ where the explicit expression for Cayley’s hyperdeterminant $D(\mathbf{a})$ is

$$\begin{aligned} D(\mathbf{a}) &= (\mathbf{a}_0\mathbf{a}_7)^2 + (\mathbf{a}_1\mathbf{a}_6)^2 + (\mathbf{a}_2\mathbf{a}_5)^2 + (\mathbf{a}_3\mathbf{a}_4)^2 - 2(\mathbf{a}_0\mathbf{a}_7)[(\mathbf{a}_1\mathbf{a}_6) + (\mathbf{a}_2\mathbf{a}_5) + (\mathbf{a}_3\mathbf{a}_4)] \\ &\quad - 2[(\mathbf{a}_1\mathbf{a}_6)(\mathbf{a}_2\mathbf{a}_5) + (\mathbf{a}_2\mathbf{a}_5)(\mathbf{a}_3\mathbf{a}_4) + (\mathbf{a}_3\mathbf{a}_4)(\mathbf{a}_1\mathbf{a}_6)] \\ &\quad + 4\mathbf{a}_0\mathbf{a}_3\mathbf{a}_5\mathbf{a}_6 + 4\mathbf{a}_1\mathbf{a}_2\mathbf{a}_4\mathbf{a}_7 \end{aligned} \quad (74)$$

giving a generalization of Eq. (73) as $S = \pi \sqrt{|-D(\mathbf{a})|}$.

Obviously the action of $\mathcal{D}(\alpha)$ on the canonical form of \mathcal{Z} by conjugation gives rise to the permutation of the charges in the form $(\mathbf{a}\mathbf{b}\mathbf{c}\mathbf{d}\mathbf{e}\mathbf{f}\mathbf{g})$. Combining this with the $PSL_2(7)$ invariance of J_4 shows that in agreement with the well-known result [4, 5, 39] the expression for J_4 in terms of the 56 charges contains (among others) the sum of seven copies of Cayley’s hyperdeterminant. These terms describe the seven different possible $N = 2, D = 4$ STU truncations of the $N = 8$ solutions. Using the explicit dictionary of Eqs. (58)–(60) we can alternatively label the points of Fig. 5 by the 28 Gaussian integers. It is easy to check that the charge configurations belonging to a particular truncation of this type correspond to seven sets of four points with mutual distance *four*.

After we have clarified the geometrical meaning of the canonical form for \mathcal{Z} , let us try to understand its symmetry properties. As already explained, we have only eight charges corresponding to the eight integers $\mathbf{a}_I, I = 0, 1, \dots, 7$. The action of the $PSL_2(7)$ subgroup of the duality group on these charges can be understood from the corresponding action on the operators c_1, e_1, f_1, g_1 (see Eqs. (61)–(62)). From Eqs. (64) and (65) we find that $\mathcal{D}(\beta)$ and $\mathcal{D}(\gamma)$, acting as $(c_1 e_1 f_1)(g_1)$ and $(c_1 f_1)(e_1)(g_1)$, generate the dihedral group D_3 , which is isomorphic to the permutation group S_3 . The action of S_3 on the eight charges in the permutation notation reads

$$\mathcal{D}(\beta) : (\mathbf{a}_0)(\mathbf{a}_7)(\mathbf{a}_3\mathbf{a}_6\mathbf{a}_5)(\mathbf{a}_1\mathbf{a}_2\mathbf{a}_4), \quad (75)$$

and

$$\mathcal{D}(\gamma) : (\mathbf{a}_0)(\mathbf{a}_7)(\mathbf{a}_1)(\mathbf{a}_6)(\mathbf{a}_2\mathbf{a}_4)(\mathbf{a}_3\mathbf{a}_5). \quad (76)$$

At this point, we get in touch with the usual interpretation based on seven three-qubit systems [4, 5]. Let us associate with the 8 charges $\mathbf{a}_I, I = 0, 1, \dots, 7$, the three-qubit state

$$|\psi\rangle \equiv \mathbf{a}_{000}|000\rangle + \mathbf{a}_{001}|001\rangle + \dots + \mathbf{a}_{111}|111\rangle, \quad (77)$$

i. e., we reinterpreted the charges \mathbf{a}_I (decimal labeling) as integer-valued amplitudes \mathbf{a}_{abc} , $a, b, c \in \{0, 1\}$ (binary labeling) of a three-qubit state. Then the transformation rules of

Eqs. (75) and (76) for the amplitudes correspond to the permutations (321) and (12) of subsystems (we are labeling qubits from left to right). Since these permutations generate the full permutation group on three letters, the corresponding truncation of J_4 (i. e., Cayley's hyperdeterminant) should be a permutation invariant, and this is indeed the case. Hence, as another important consistency check, we reproduced the permutation invariance of Cayley's hyperdeterminant from the $PSL_2(7)$ symmetry of Cartan's quartic invariant.

7 Conclusion

We have performed a comprehensive analysis of the properties of the *real* generalized Pauli operators of three-qubits to the extent comparable with the treatment of the (complex) two-qubit case [15, 16]. The algebra of the operators is found to be completely describable in terms of the structure of the Fano plane and uniquely extendible to the picture of the split Cayley hexagon of order two. The 63 Pauli operators are bijectively identified with 63 points of the Hexagon whose 63 lines carry each triples of operators; these triples are such that the product of any two of them gives, up to a sign, the third one. A deeper insight into the structure of the Hexagon is acquired in terms of one of its automorphism of order 7 that features 9 orbits of 7 points/operators each. The factorization of the set of operators into 35 symmetric and 28 antisymmetric members finds its natural explanation in terms of two distinct kinds of points of the Hexagon: 7 Fano points, 7 Fano lines and 21 Fano flags on the one hand versus 28 Fano anti-flags on the other hand, respectively. Triples of collinear operators are of two distinct kinds as well, according as they lie on the lines of point/line/flag (Heawood) type or on those of flag/anti-flag/anti-flag (Coxeter) type. The geometry behind 28 antisymmetric matrices is governed by the properties of the Coxeter graph and its symmetries. The geometry behind 21 out of 35 symmetric guys rests on the Heawood graph, while that of the full set is mimicked by a Klein quadric in a projective 5-space over $GF(2)$.

Employing this novel finite geometrical language, an alternative quantum informational view of the structure of the E_7 -symmetric black hole entropy formula and a subgroup of its duality symmetry has been arrived at. This view is based on the *algebra of observables on three-qubits*. This is to be contrasted with the other ones [4, 5] based on *an entangled state of seven qubits*. In both pictures, however, three-qubits play a distinguished role. We managed to establish a dictionary between these complementary approaches. However, there are still many questions left to be answered. The most exciting one is the possibility of relating the black hole entropy formula to the *full geometry of the Hexagon*. Indeed, we only managed to relate black hole solutions to the Coxeter sub-geometry with an explicit $PSL_2(7)$ symmetry. We conjecture that the full $G_2(2)$ symmetry of the Hexagon should play a role in this black hole context. One solid piece of evidence in favour of this conjecture is the fact that since E_7 is of rank seven we have $133 - 7 = 2 \times 63 = 126$ step operators. According to an important result of M. Koca and his co-workers [40], the adjoint Chevalley group $G_2(2)$ acts naturally on the (octonionic) root system of E_7 . Using this result and our explicit dictionary, it would be really spectacular to establish a full correspondence between the geometry of the Hexagon and the duality symmetries of stringy black hole solutions.

As already remarked, there exist two distinct generalized hexagons of order two: our Hexagon and its dual. One is naturally tempted to ask why three-qubits favour the former, not the latter. Since the algebra of the corresponding operators is encoded in the structure of the Fano plane, the answer seems to be rather easy: our Hexagon, as we have seen, contains a sub-hexagon of order (1, 2) which is isomorphic to the incidence graph of the Fano plane, but its twin does not. Yet, there exists another remarkable structure within our Hexagon which is absent in its counterpart, a *distance-2-ovoid* [18]–[22]. A distance-2-ovoid is a set of non-collinear points such that every line is incident with exactly one point of that set and for a generalized hexagon of order (s, t) its cardinality amounts to $s^2t^2 + st + 1$. In our Hexagon, this is the *unique* configuration of 21 points of flag type (orange, red and pink circles in Fig. 4). Why we should be bothered with this set? Because generalized hexagons and their sub-configurations have recently been found to be an important source of a variety of *codes* [41], with those arising from distance-2-ovoids being of specific two-weight type.

This link with coding theory is something which certainly deserves a serious perusal of its own.

As a final note, we would like to draw the reader's attention to the following puzzling analogy. We have already mentioned in the introduction that multi-qubit states of smallest orders can geometrically be modelled by Hopf fibrations. Namely, the k -qubit states, $k = 1, 2, 3$, are intimately connected with the Hopf sphere fibrations of the

$$S^{2^{(k+1)}-1} \xrightarrow{S^{2^k-1}} S^{2^k}$$

type, respectively [11, 13]. A very similar situation occurs in the setting provided by thick generalized n -gons. For if we associate the geometry of three non-trivial matrices given by Eq. (3) with that of the generalized digon ($n = 2$) of order two, and take into account that the two-qubit case is underlaid by the geometry of the generalized quadrangle ($n = 4$) of order two [15, 16], we also arrive at such a three-fold correspondence: $n = 2k$, $k = 1, 2, 3$. Moreover, in both the cases, remarkably, the sequence ends at $k = 3$; in the former case due to the fact that there are no natural Hopf fibrations of higher order, whilst in the latter one because, by the celebrated result of Feit and Higman [42], of non-existence of thick generalized n -gons with $n > 6$ and meeting the constraint $s = t$. We thus observe a fascinating phenomenon when two substantially different pieces of mathematics convey the same message: a special footing played by single-qubit, two-qubit and three-qubit systems within an infinite family of multiple-qubit states. Is this analogy a mere coincidence, or is there a deep physical reason behind?

Acknowledgements

One of us (P.L.) would like to express his gratitude to professor Michael Duff for the warm hospitality during his recent stay at the Imperial College in London. His special thanks also go to Leron Borsten and Duminda Dahanayake for useful correspondence. This work was partially supported by the VEGA grant agency projects Nos. 6070 and 7012. We are extremely grateful to our friend Petr Prajna (Prague) for creating the electronic versions of all the figures.

References

- [1] M. J. Duff, Phys. Rev. D **76**, 025017 (2007).
- [2] R. Kallosh and A. Linde, Phys. Rev. D **73**, 104033 (2006).
- [3] P. Lévay, Phys. Rev. D **74**, 024030 (2006); P. Lévay, Phys. Rev. D **76**, 106011 (2007).
- [4] S. Ferrara and M. J. Duff, Phys. Rev. D **76**, 025018 (2007).
- [5] P. Lévay, Phys. Rev. D **75**, 024024 (2007).
- [6] S. Ferrara and M. J. Duff, Phys. Rev. D **76**, 124023 (2007).
- [7] L. Borsten, D. Dahanayake, M. J. Duff, H. Ebrahim, and W. Rubens, Phys. Rev. Lett. **100**, 251602 (2008).
- [8] M. J. Duff, J. T. Liu, and J. Rahmfeld, Nucl. Phys. B **459**, 125 (1996).
- [9] K. Behrndt, R. Kallosh, J. Rahmfeld, M. Shmakova, and W. K. Wong, Phys. Rev. D **54**, 6293 (1996).
- [10] V. Coffman, J. Kundu, and W. Wootters, Phys. Rev. A **61**, 052306 (2000).
- [11] R. Mosseri and R. Dandoloff, J. Phys. A **34**, 10243 (2001).
- [12] P. Lévay, J. Phys. A **37**, 1821 (2004).
- [13] B. A. Bernevig and H.-D. Chen, J. Phys. A **36**, 8325 (2003).
- [14] M. Saniga and M. Planat, Adv. Studies Theor. Phys. **1**, 1 (2007).
- [15] M. Saniga, M. Planat, and P. Prajna, Theor. Math. Phys. **155**, 905 (2008).
- [16] M. Planat and M. Saniga, Quant. Inform. Comput. **8**, 127 (2008).
- [17] H. Havlicek, A mathematician's insight into the Saniga-Planat theorem, invited lecture, Finite Projective Geometry in Quantum Theory, Tatranská Lomnica, Slovakia, August 2, 2007; <http://www.geometrie.tuwien.ac.at/havlicek/slides/tatra2007.pdf>

- [18] B. Polster, *Discr. Math.* **256**, 373 (2002).
- [19] A. E. Schroth, *Discr. Math.* **199**, 161 (1999).
- [20] B. Polster, A. E. Schroth, and H. Van Maldeghem, *Math. Intelligencer* **23**, 33 (2001).
- [21] B. Polster, *A Geometrical Picture Book* (Springer, New York, 1998).
- [22] H. Van Maldeghem, *Generalized Polygons* (Birkhäuser, Basel, 1998).
- [23] W. Dür, G. Vidal, and J. I. Cirac, *Phys. Rev. A* **62**, 062314 (2000).
- [24] M. A. Nielsen and I. L. Chuang, *Quantum Computation and Quantum Information* (Cambridge University Press, Cambridge, 2000).
- [25] J. Baez, *Bull. Amer. Math. Soc.* **39**, 145 (2002).
- [26] A. M. Cohen and J. Tits, *Europ. J. Combinatorics* **6**, 13 (1985).
- [27] J. A. Thas and H. Van Maldeghem, *Finite Fields and Their Applications* **12**, 565 (2006).
- [28] H. Van Maldeghem, *Atti Semin. Mat. Fis. Univ. Modena* **48**, 463 (2000).
- [29] G. Pickert, *Math. Semesterber.* **29**, 51 (1982).
- [30] J. W. P. Hirschfeld, *Finite Projective Spaces in Three Dimensions* (Oxford University Press, Oxford, 1985).
- [31] J. H. Conway and N. J. A. Sloane, *Sphere Packings, Lattices and Groups* (Springer-Verlag, New York, 3rd Edition, 1999) p. 267.
- [32] H. S. M. Coxeter, *Proc. London Math. Soc.* **46**, 117 (1983).
- [33] R. Kallosh and B. Kol, *Phys. Rev. D* **53**, R5344 (1996).
- [34] E. Cartan, *Ouvres Completes* (Editions du Centre National de la Recherche Scientifique, Paris, 1984).
- [35] K. Becker, M. Becker, and J. H. Schwarz, *String Theory and M-Theory* (Cambridge University Press, Cambridge, 2007) p. 576.
- [36] E. Cremmer and B. Julia, *Nucl. Phys. B* **159**, 141 (1979).
- [37] V. Balasubramanian, F. Larsen, and R. G. Leigh, *Phys. Rev. D* **57**, 3509 (1998); M. Gunaydin, K. Koepsell, and H. Nicolai, *Commun. Math. Phys.* **221**, 57 (2001).
- [38] L. Borsten, D. Dahanayake, M. J. Duff, H. Ebrahim and W. Rubens, in preparation.
- [39] L. Manivel, *Journal of Algebra* **304**, 457 (2006) (arXiv:math.AG/0507118).
- [40] F. Karsch and M. Koca, *J. Phys. A* **23**, 4739 (1990); M. Koca, R. Koc, and N. Ö. Koca, arXiv:hep-th/0509189.
- [41] A. De Wispelaere and H. Van Maldeghem, *Des. Codes Cryptogr.* **37**, 435 (2005).
- [42] W. Feit and G. Higman, *J. Algebra* **1**, 114 (1964).